Ref.TH.2009-CERN

THE KINEMATIC AND SYMMETRY STRUCTURE OF $e^+e^- \rightarrow$ HADRON PAIRS

F. E. Close
CERN - Geneva

and

W.N. Cottingham
University of Bristol, England

A B S T R A C T

The kinematic singularity and constraint free amplitudes for $e^+e^- \rightarrow$ two particles which can have arbitrary spins are obtained in a simple closed form. The relationships of these amplitudes with the usual multipole form factors are given. It is noted that $SU(6)_W$ and tests of ideas based on the Melosh transformation are liberated from their γN and πN arena and can be confronted with arbitrary targets and excitations. The matrix elements for arbitrary meson pairs are then derived, rates are computed for pseudoscalar and vector meson production, and some tests of symmetry breaking mechanisms proposed. Extension to $SU(4)[SU(8)_W]$ broken in the masses enables estimates of charmed particle production rates to be obtained. General features of πR final states suggest that scaling violation at small x may be connected with threshold phenomena as channels open up. A subtle difference between spacelike and timelike regions is highlighted.

Ref.TH.2009-CERN
2 April 1975

CONTENTS

INTRODUCTION

During the next few years an increasing amount of activity is anticipated in the field of e^+e^- annihilation. The interest in this field is already well established commencing with the vector mesons seen at Orsay, the large cross-sections discovered at Frascati and CEA[1] recently supplemented by the discovery of hitherto unexpected states found at SPEAR, Frascati and DORIS[2].

After the initial surveys of total and inclusive cross-sections a fruitful area of study will be the channels that build up the total cross-section. For $t < 9(\text{GeV})^2$ there have already been some first investigations along these lines at Frascati [1, 3] and with D. C. I. soon to cover this same energy range we anticipate much interest in such phenomena. If heavy states with new quantum numbers are discovered (e. g. charm or states associated with the new heavy bosons) then we may even anticipate studies of exclusive channels at SPEAR-DORIS energies.

In view of these expected developments we have made a study of quasi two body production in e^+e^- annihilation in order to clarify some of the interesting questions for experiment to investigate. Our work complements and extends earlier work of various authors [4-7].

In section 2 we discuss kinematics, in particular we show how to define kinematic singularity and constraint free form factors for $e^+e^- \rightarrow$ two body systems with arbitrary spins. This goes significantly beyond previous discussions of which the most extensive to date has been that of ref. 4. Our approach is to use the formalism developed by T. L. Trueman[8], cross to the annihilation channel and boost to the e^+e^- c.m. frame. We notice that certain general features systematically arise in the t dependence of various channels which may shed some light on phenomena seen in the inclusive data. Also some observations are made on the differences between the spacelike and timelike regions which give further insight into the different behaviour vis-a-vis scaling, in these two regions.

In section 2 we discuss the application of $SU(6)_w$ and the Melosh transformation to the matrix elements $\mathcal{J} \rightarrow 1, 2$ where 1 and 2 are members of SU(6) supermultiplets. This, combined with the formalism developed in section 1 enables us to compute magnitudes for various channel cross-sections. This will be of use in planning experiments and in comparing their results. This is of particular interest because of the extensive phenomenological

successes of symmetry calculations, based on the Melosh transformation, applied to γp, γn and πN transitions in the resonance region[9]. In the timelike region one will be able to test these ideas as a function of t in $e^+e^- \to pX$ and in addition in $e^+e^- \to 1, 2$ extend the domain of application to arbitrary targets and excitations. Quasi two body e^+e^- annihilation will be an excellent theatre for further confrontation of extended symmetry predictions.

We also discuss the effects that arise if SU(3) symmetry is broken only by masses. Such breaking has consequences which can readily be examined in e^+e^- collisions. We see that e^+e^- annihilation is a nice laboratory for investigating symmetry breaking effects[10].

As an application of our results we discuss in section 3.4 the question whether the enhancement in $e^+e^- \to \pi^+\pi^-\pi^o\pi^o$[3] is a threshold phenomenon or a $\rho'(1250)$ resonance. Some consequences of various hypotheses are examined and further experimental tests proposed.

1. KINEMATICS, CONSTRAINT FREE AMPLITUDES AND THE MULTIPOLE EXPANSION FOR QUASI TWO BODY PRODUCTION

1.1 Kinematics

The e^+e^- annihilation cross section through one photon into particles 1 and 2 with helicities λ_1 and λ_2 can be written

for $\mu = \lambda_{e^-} - \lambda_{e^+} = \pm 1$

$$\frac{d\sigma}{d\Omega} = \frac{\alpha^2 p}{t^{5/2}} \left| d^1_{\mu\lambda}(\theta) \Gamma_{\lambda_1\lambda_2} \right|^2 \qquad (1.1)$$

where

$$\lambda = \lambda_1 - \lambda_2 \qquad (1.2)$$

θ = angle between the direction of particle 1 and the electron beam direction

p = magnitude of particle 1 momentum $\equiv \frac{m_1 m_2}{\sqrt{t}} \sinh\zeta$

$t = 4 * (\text{Beam energy})^2$

and $\Gamma_{\lambda_1\lambda_2}$ is the Lorentz covariant matrix element

$$\Gamma_{\lambda_1\lambda_2} = \frac{2\sqrt{E_1E_2}}{e} \left\langle \lambda_1\lambda_2\, p \left| j_\lambda(0) \right| 0 \right\rangle \qquad (1.3)$$

where $j_\lambda(0)$ is the electromagnetic current operator

$$j_{\pm 1}(0) = \mp (j_x \pm i j_y) / \sqrt{2} \qquad (1.4)$$

$$j_o(0) = j_z$$

and the z axis is the direction of the three momentum of particle 1.

Similarly one can write the cross-section for e^+e^- annihilation with $\mu = 0$. However this is smaller than that for $\mu = \pm 1$ by a factor m_e^2/t (m_e = electronmass) and we shall not consider this small cross-section further in this work.

Discrete symmetries place constraints on the $\Gamma_{\lambda_1\lambda_2}$. Parity conservation gives the relation

$$\Gamma_{\lambda_1\lambda_2} = \eta_1\eta_2 \, (-1)^{s_1 + s_2} \quad \Gamma_{-\lambda_1-\lambda_2} \tag{1.5}$$

where $\eta_{1,2}$ are the intrinsic parities of the pair. If, in addition, 2 is the antiparticle of 1, then charge conjugation invariance gives the relation

$$\Gamma_{\lambda_1\lambda_2} = \Gamma_{-\lambda_2-\lambda_1} \tag{1.6}$$

1.2 Constraint Free Amplitudes

To decompose the current matrix elements into form factors which are free of kinematic singularities and constraints we employ the method of Trueman[8]. First define

$$\Gamma_{\lambda_1\lambda_2} = \frac{2\sqrt{E_1E_2}}{e} \left\langle \lambda_2, \xi \left| j_\lambda(0) \right| -\lambda_1 \right\rangle' \tag{1.7}$$

where

$\left| -\lambda_1 \right\rangle'$ is the antiparticle of 1 at rest and with spin projection $-\lambda_1$ along the z axis;

$|\lambda_2, \xi\rangle$ is particle 2 with helicity λ_2 moving along the -z axis with rapidity

The rapidity is related to the invariant momentum transfer t by

$$\cosh\left(\tfrac{1}{2}\xi\right) = \left[\frac{(m_1+m_2)^2 - t}{4 m_1 m_2}\right]^{\frac{1}{2}}$$
$$\sinh\left(\tfrac{1}{2}\xi\right) = \left[\frac{(m_1-m_2)^2 - t}{4m_1m_2}\right]^{\frac{1}{2}} \qquad (1.8)$$

$\Gamma_{\lambda_1\lambda_2}$ describes the decay (or excitation) of the antiparticle of 1 into 2 with the emission (or absorption) of a real or virtual photon, the physical region for such processes being

$t < (m_1-m_2)^2$.

Γ' is related to Γ by first crossing 1 into the production channel (implying analytic continuation in t to $t > (m_1+m_2)^2$) ; this is followed by a Lorentz transformation to the centre of mass system. For $\lambda = \pm 1$ this gives the relationship

$$\Gamma_{\lambda_1\lambda_2} = \Gamma'_{\lambda_1\lambda_2} \qquad (\lambda_1 = \lambda_2 \pm 1) \qquad (1.9)$$

and for $\lambda = 0$ (remembering that charge conservation relates the timelike and spacelike current components)

$$\Gamma_{\lambda_1\lambda_2} = \frac{2m_1\sqrt{t}}{t-m_2^2+m_1^2}\,\Gamma'_{\lambda_1\lambda_2} \quad (\lambda_1 = \lambda_2) \qquad (1.10)$$

The method of Trueman[8] applied to the matrix elements Γ' shows that the amplitudes $T^s_i(t)$ defined by

$$T_\ell^s(t)\ (\sinh\tfrac{1}{2}\xi)^{|s_2-s|+\ell}\ (\cosh\tfrac{1}{2}\xi)^{s_2+s-\ell}$$

$$= \sum_{\lambda_1\lambda_2} \langle s_1, 1, \lambda_1, \lambda_2-\lambda_1 \,|\, s, \lambda_2\rangle\ d^L_{L-\ell,\,\lambda_2}(\tfrac{\pi}{2})\ d^{L'}_{L',\lambda_2}(\tfrac{\pi}{2})\ \Gamma'_{\lambda_1\lambda_2} \qquad (1.11)$$

(where $L = \min(s_2, s)$, $L = \max(s_2 s)$)

are free of kiematic singularities in both the direct and crossed channels. They are also a complete set of amplitudes and, apart from charge conjugation invariance when 1 and 2 are particle antiparticle pairs, they are independent. There is also the important reciprocal relationship

$$\Gamma'_{\lambda_1\lambda_2} = \sum_{s\ell} \frac{d^L_{L-\ell,\,\lambda_2}(\frac{\pi}{2})}{d^{L'}_{L'\lambda_2}(\frac{\pi}{2})} \langle s_1, 1, \lambda_1, \lambda_2-\lambda_1 \,|\, s, \lambda_2\rangle\ T^s_\ell(t)(\sinh\tfrac{1}{2}\xi)^{|s_2-s|+\ell}$$

$$(\cosh\tfrac{1}{2}\xi)^{s_2+s-\ell} \qquad (1.12)$$

Parity conservation, with Eq. (1.12), gives the simple restriction that $T^s_\ell(t) = 0$ if $(-1)^\ell = \eta_1\eta_2(-1)^{s_2+s}$.

Charge conjugation invariance gives no further restriction for $\lambda_1 = \lambda_2$. Otherwise Eq. (1.6) gives s_1 contraints for boson particle antiparticle pair creation and $s_1-\frac{1}{2}$ constraints for fermion pair creation.

1.3 The Multipole Expansion

Consider the covariant matrix element

$$\frac{2\sqrt{E_1 E_2}}{e} \left\langle \lambda_2 \zeta \left| j_{-\mu}(0)\ R^{+}\ (\varphi, \theta, 0) \right| m_1 \right\rangle' = A'^{\mu}_{m_1 \lambda_2}(\zeta, \theta\varphi) \quad (1.14)$$

which, for example, could describe the state $\bar{1}$ at rest and with spin projection m_1 along the z axis decaying into a "photon" of helicity μ moving in the direction specified by the polar angles $\theta\varphi$ and the state 2 with helicity λ_2, rapidity ζ in the opposite direction. Clearly

$$A'^{\mu}_{m_1, \lambda_2}(\zeta\ \theta, \varphi) = \Gamma'_{\lambda_2 - \mu,\ \lambda_2}\ \mathcal{D}^{s_1}_{\lambda_2 - \mu,\ -m_1}(0\,\theta\varphi) \quad (1.15)$$

Suppose that the spin of particle 2 is specified not by helicity but by its projection m along the z axis in its rest frame. It is easy to show that the corresponding matrix element is

$$A^{\mu}_{m_1 m_2}(\theta, \varphi) = \sum_{\lambda_2} \mathcal{D}^{s_2}_{m_2, -\lambda_2}(\varphi, \theta, 0)\ A'^{\mu}_{m_1, \lambda_2}$$

$$= \sum_{\lambda_2} (-1)^{m+\lambda_2}\ \mathcal{D}^{s_2}_{-\lambda_2, m_2}(0, \theta, \varphi)\ \mathcal{D}^{s_1}_{\lambda_2 - \mu, -m_1}(0\theta\varphi)\ \Gamma'_{\lambda_2 - \mu, \lambda_2}\,. \quad (1.16)$$

Using the theorem on the product of $\mathcal{D}$ functions, and the rearrangement theorem of Clebsch Gordan coefficients [11] this can be expressed as

$$A^{\mu}_{m_1 m_2}(\theta, \varphi) = \sum_{j} \mathcal{D}^{j*}_{m_1 - m_2, \mu}(\varphi, \theta, 0)\ \left\langle s_2, m_2, j, m_1 - m_2 \right| \left. s_1, m_1 \right\rangle g^{j}_{\mu} \quad (1.17)$$

where

$$g^j_\mu = \sqrt{\frac{2j+1}{2s_1+1}} \sum_{\lambda_2} (-1)^{s_2+\lambda_2} \left\langle s_2, -\lambda_2, s_1, \lambda_2-\mu \,\middle|\, j, -\mu \right\rangle \Gamma_{\lambda_2-\mu, \lambda_2} \qquad (1.18)$$

For the cases $\mu = \pm 1$ (eq. (1.17) is a relativistic generalisation of the multipole expansion [11], with moments g^j_μ.

Parity conservation gives the relationship

$$g^j_{-\mu} = \eta_1\eta_2(-1)^j g^j_\mu \qquad (1.19)$$

The index j can be taken to specify the total angular momentum of the "photon" (real or virtual). For $\mu = \pm 1$ the functions $g^j_\mu(s)$ can be used to define multipole form factors of order 2^j; electric when $g^j_\mu = g^j_{-\mu}$ and magnetic when $g^j_\mu = -g^j_{-\mu}$ [11]. The functions $g^j_o(s)$ can be used to define "charge" multipole form factors.

1.4 Examples

(i) 1 and 2 are π^- and π^+

There is only one helicity amplitude which can be expressed in terms of the usual electric form factor[12]

$$\Gamma'_{oo} = g^o_o = -2m_\pi G_E(t) (\sinh \tfrac{1}{2}s)(\cosh \tfrac{1}{2}s) \qquad (1.20)$$

The invariant form factor as defined here is

$$T_o(t) = \sqrt{2m_\pi}\, G_E(t) \qquad (1.21)$$

See also section 2.5 for arbitrary pseudoscalar meson pairs production.

(ii) 1 and 2 are $\bar{p}$ and p

There are two helicity amplitudes which are related to the usual electric and magnetic form factors [13] by

$$\Gamma'_{\frac{1}{2}\frac{1}{2}} = \Gamma'_{-\frac{1}{2}-\frac{1}{2}} = g^{o}_{o} = -2M\, G_E(t) \sinh \tfrac{1}{2}\xi \qquad (1.22)$$

$$\Gamma'_{-\frac{1}{2}\frac{1}{2}} = \Gamma'_{\frac{1}{2}-\frac{1}{2}} = -\sqrt{\frac{3}{2}}\, g^{1}_{1} = +2M \sqrt{2}\, G_M(t) \sinh \tfrac{1}{2}\xi \qquad (1.23)$$

The invariant form factors as defined here are

$$T^{\frac{1}{2}}_{1}(t) = \frac{2M}{\sqrt{3}} \left(G_E(t) + 2G_M(t) \right) \qquad (1.24$$

$$T^{3/2}_{o}(t) = \frac{2M}{\sqrt{2}\cosh^2 \frac{1}{2}\xi} \left(G_E(t) - G_M(t) \right) \qquad (1.25)$$

These are singularity free and at $t = 4m^2$, where $\cosh\frac{1}{2}\xi = 0$, the well known constraint $G_E(4m^2) = G_M(4m^2)$ is seen.

(iii) 1 and 2 are ω^o and π^o

Again there is one helicity amplitude for this magnetic dipole transition. We can define a magnetic dipole form factor by

$$\Gamma'_{10} = -\Gamma'_{-10} = -g^{1}_{1} = 2m_{\pi} G_M(t) \sinh(\tfrac{1}{2}\xi) \cosh(\tfrac{1}{2}\xi) \qquad (1.26)$$

and then

$$T^{1}_{o}(t) = -2m_{\pi} G_M(t)$$

See also section 2.6 for pseudoscalar-vector production.

(iv) 1 and 2 are R and π

If R is any natural parity meson, with spin s, then there is only one helicity amplitude $\Gamma'_{10} = -\Gamma'_{10}$ and we have

$$T_o^{s_1}\left[\sinh(\tfrac{1}{2}\xi)\cosh(\tfrac{1}{2}\xi)\right]^{s_1} = \frac{\sqrt{2(2s_1)!}}{(s_1!)\,2^{s_1}}\,\Gamma'_{10}\,(-1)^s \qquad (1.28)$$

This example is discussed in section 4.

If R has unatural parity then there are two helicity amplitudes which are straightforward to obtain from our general formalism.

(v) 1 and 2 are ρ^- and ρ^+

For the general vector-vector transition there are four independent amplitudes

$$\Gamma'_{11} = \Gamma'_{-1-1};\quad \Gamma'_{00};\quad \Gamma'_{01} = \Gamma'_{0-1};\quad \Gamma'_{10} = \Gamma'_{-10} \qquad (1.29$$

and four form factors, However for this particular case the charge conjugation constraint $\Gamma'_{01} = \Gamma'_{10}$ recuces the independent amplitudes to three. These can be taken as

$$T_1^1 \sinh\tfrac{1}{2}\xi\,\cosh\tfrac{1}{2}\xi = \tfrac{1}{2}(\Gamma'_{11} - \Gamma'_{01}) \qquad (1.30)$$

$$T_2^2(\sinh\tfrac{1}{2}\xi)^3\cosh\tfrac{1}{2}\xi = \frac{1}{2\sqrt{2}}(\Gamma'_{00} - \Gamma'_{11}) \qquad (1.31)$$

$$T_o^2 \sinh\tfrac{1}{2}\xi\,(\cosh\tfrac{1}{2}\xi)^3 = \frac{1}{2\sqrt{2}}(\Gamma'_{00} + \Gamma'_{11} + 2\Gamma'_{01}) \qquad (1.32)$$

In terms of the multipole form factors of section 1 and reference 13

$$g_o^o = 2m\rho F_E \sinh\tfrac{1}{2}\zeta \cosh\tfrac{1}{2}\zeta = \frac{1}{3}(\Gamma'_{00} + 2\Gamma'_{11}) \qquad (1.33)$$

$$g_1^1 = -\sqrt{2}\,2m\rho F_M \sinh\tfrac{1}{2}\zeta \cosh\tfrac{1}{2}\zeta = -\sqrt{2}\,\Gamma'_{01} \qquad (1.34)$$

$$g_o^2 = \frac{4\sqrt{10}}{3} m\rho F_Q (\sinh\tfrac{1}{2}\zeta)^3 \cosh\tfrac{1}{2}\zeta = \frac{\sqrt{10}}{3}(\Gamma'_{11} - \Gamma'_{00}) \qquad (1.35$$

Again note how Eq. (1.32) constrains these multipole form factors at $\cosh\left(\frac{1}{2}\zeta\right) = 0$ $(t = 4m^2)$.

2. $SU(6)_w$ SYMMETRY AND CURRENT-CONSTITUENT QUARK CONSTRAINTS ON TWO BODY PRODUCTION AMPLITUDES

Introduction

During the last two years there have been significant advances in the phenomenology of resonance region physics based upon the transformation between current and constituent quarks[14]. A wide range of successful applications of these ideas has been made in the cases where electromagnetic and pion "currents" (through P. C. A. C.) interact with the nucleon and excite various resonant states [9, 15, 16].

Electron-positron annihilation into hadrons via a single photon is an excellent arena for testing these ideas in a rich variety of

new ways. First, in $e^+e^- \to \bar{p}N^*$ one can choose various N^* to accompany the $\bar{p}$ and see how well the theory continues to work as t is varied in the timelike domain. Second, and potentially more exciting, is the liberation from the restriction to nucleon targets since in $e^+e^- \to 1, 2$ one has all possible cross channel targets.

Here we give the general $SU(6)$ structure of the matrix elements when 1, 2 are arbitrary mesons. Data are not yet of quality enough to confront with these results. However we consider in some detail the cases where 1, 2 belong to the lowest super-multiplet and compute various cross-sections which should be compared with experiment in the near future.

2.1. $SU(6)_w$ constraints on $e^+e^- \to$ two body systems

The $SU(6)_w$ constraints on $e^+e^- \to \gamma \to 1, 2$ are related to those for $\gamma\, \bar{1} \to 2$. If the transformation properties of the states 1 and 2 under $SU(6)_w$ strong are specified then all that is needed for the calculation are the transformation properties of the electromagnetic current under $SU(6)_w$ strong.

If we assume that the current belongs to a SU(3), $\underset{\sim}{8}$ part of a 35 plet (or equivalently in quark language restrict the current to interact with a single constituent quark*) then the most general form of the current under $\left[SU(6)_w \otimes O(2)_{L_z}\right]$ is as follows.

For a transverse photon with $J_z = +1$ the electromagnetic interaction operator can be formally written (14, 15, 16)

$$J_T^+ = (Av_+ + B\sigma_+ + Cv_+\sigma_z + Dv_+v_+\sigma_-)\, I \qquad (2.1)$$

while for a longitudinal photon ($J_z = 0$) one has[16]

$$J_L^{(o)} = (\alpha + \beta(\sigma_- v_+ + \sigma_+ v_-))I \qquad (2.2)$$

In these relations $v_{\pm}$ are orbital angular momentum raising, lowering, operators according to their index and we have factored the current

---

* The relationship between current and constituent quarks, $SU(6)_w$ strong, current and a general introduction to the ideas of the Melosh transformation[17] are given in the lectures of Weyers ref. 14. See also refs. 9, 16 for subsequent developments and the discussion leading to Eqs. (2.1), (2.2) of the present text.

operator into a spin orbit part (in parenthesis) and an SU(3) octet operator I.[x] The A, α etc. are SU(6) singlet operators.[y]

As in previous work we consider the SU(6) symmetry of $\Gamma'_{\lambda_1\lambda_2}$ rather than $\Gamma_{\lambda_1\lambda_2}$. The application to $e^+e^- \to 1, 2$ is by crossing Eq. (1.9) and (1.10). (It should be noted that $[SU(6)_w \otimes O(2)_{L_z}]$ is a collinear symmetry invariant under boosts along the z direction and hence ideal for this transformation). The combination of these matrix elements with the general structure of section 1. enables relations to be obtained between various cross sections and will be illustrated in section 3.

Suppose that the state 1 which has total spin s_1 is made up of quarks in a state with intrinsic spin S_1 (= 0 or 1) and orbital angular momentum L_1, (similarly the state 2). One then obtains

---

x The extension to include charm is trivial. I becomes an SU(4) 15 plet operator, the spin orbit part being unchanged.

y In a quark model these quantities depend upon quark masses, binding potentials, etc. Some attempt at discussing the structure of these quantities is given in ref. 18.

(i) Transverse photon $\lambda = \lambda_1 - \lambda_2 = -1$

$$\Gamma'_{\lambda_1\lambda_2} = \sum_{L_z} \langle L_2 \delta_2, L_z \delta_{2z} | s_2, \lambda_2 \rangle \gamma_{-1}^{L_z} \; [SU(3)] \qquad (2.3)$$

$$\gamma_{-1}^{L_z} = \left\{ \begin{array}{l} A^{L_z} \langle L_1 \delta_1, L_z - 1, \delta_{1z} | s_1, \lambda_1 \rangle \; \delta_{W_1 W_2} \\ + B^{L_z} \langle L_1 \delta_1, L_z \; \delta_{1z} - 1 | s_1, \lambda_1 \rangle \langle W_2 W_z | \sigma^+ | W_1, W_z - 1 \rangle \\ + C^{L_z} \langle L_1 \delta_1, L_z - 1, \delta_{1z} | s_1, \lambda_1 \rangle \langle W_2 W_z | \sigma^z | W_1, W_z \rangle \\ + D^{L_z} \langle L_1 \delta_1, L_z - 2, \delta_{1z} + 1 | s_1, \lambda_1 \rangle \langle W_2 W_z | \sigma^- | W_1, W_z + 1 \rangle \end{array} \right\}$$

(ii) Longitudinal photon $\lambda = \lambda_1 - \lambda_2 = 0$

$$\Gamma'_{\lambda_1\lambda_2} = \sum_{L_z} \langle L_2 \delta_2, L_z \; \delta_{2z} | s_2 \lambda_2 \rangle \gamma_0^{L_z} \; [SU(3)] \qquad (2.4)$$

$$\gamma_0^{L_z} = \left\{ \begin{array}{l} \alpha^{L_z} \langle L_1 \delta_1, L_z \delta_{1z} | s_1 \lambda_1 \rangle \; \delta_{W_1 W_2} \\ + \beta^{L_z} \langle L_1 \delta_1, L_z - 1, \delta_{1z} + 1 | s_1 \lambda_1 \rangle \langle W_2 W_z | \sigma^- | W_1, W_z + 1 \rangle \\ + \beta^{L_z} \langle L_1 \delta_1, L_z + 1, \delta_{1z} - 1 | s_1 \lambda_1 \rangle \langle W_2 W_z | \sigma^+ | W_1, W_z - 1 \rangle \end{array} \right\}$$

The A^{L_z}, α^{L_z} etc. are SU(6) invariants but do depend on the orbital quantum numbers of the states 1 and 2. The only subtlety

in the use of these formulae is in the distinction between W spin and ordinary spin in the J L S coupling scheme[13].

The spinor matrix elements in Eqs. (2.3) (2.4) are listed in Table 1 and the SU(3) factors in Table 2. An extension of this formalism to include charm is given in Table 3.

3. Pair production of mesons in the L = 0 supermultiplet

In the lowest supermultiplet with $L_1 = L_2 = 0$, s_1 and s_2 can be 0^- and 1^-. Typical examples of such mesons are the π, ρ, K etc. and as these are the least massive hadrons one may expect that their production in pairs will be an important feature of the low energy hadron production cross section. We use the formalism of sections 1 and 2 to estimate rates for such pair production.

In this case the general structure of Eq. (2.3 and 2.4) simplifies considerably. Eq. (2.3) for transverse photons becomes

$$\Gamma'_{\lambda_2 -\lambda_2} = B^{oo} \left\langle W_2, W_{2z} \left| \sigma_+ \right| W_1, W_{1z} - 1 \right\rangle \left[SU(3)\right] \qquad (3.1)$$

while for longitutinal photons Eq. (2.4) gives

$$\Gamma'_{\lambda_1 \lambda_1} = \alpha^{oo} \delta_{w_1 w_2} \left[SU(3)\right] \qquad (3.2)$$

Hence the excitations of pairs from this supermultiplet are given in terms of two reduced matrix elements B^{oo} and α^{oo} which are the expectation values of the SU(6) singlet operators

B and α (Eq. 2.1 and 2.2) taken between states with $L_1 = L_2 = 0$.

For vector (V) and pseudoscalar meson (P) production the results for the helicity amplitudes follow immediately from Eq. (3.1) and Eq. (3.2) with Table 1.

$$P\ P \qquad \Gamma'_{00} = \alpha^{00}\ [SU(3)] \tag{3.3}$$

$$V\ P \qquad \Gamma'_{00} = 0$$

$$\Gamma'_{10} = \frac{1}{\sqrt{2}}\ B^{00}\ [SU(3)] \tag{3.4}$$

$$V\ V \qquad \Gamma'_{00} = \Gamma'_{11} = \alpha^{00}\ [SU(3)] \tag{3.5}$$

$$\Gamma'_{01} = \Gamma'_{-10} = \frac{-1}{\sqrt{2}}\ B^{00}\ [SU(3)] \tag{3.6}$$

The connection with the formalism of section 1 is complete if we identify

$$\begin{aligned} \alpha^{00}\ [SU(3)] &= -\,p'\,G_E \\ 1/\sqrt{2}\ B^{00}\ [SU(3)] &= -\,p'\,G_M \end{aligned} \tag{3.7}$$

where $p' = m_2 \sinh\xi$ is the momentum of particle 2 in this system. There is a problem now with the explicit broken symmetry of the masses. The problem occurs with the SU(3) properties of other vertex functions and there it is known that the symmetry predictions have most phenomenological success when explicit kinematic momenta are removed. We do this here and identify

$$G_E^{\pi\pi} = G_E^{\rho\rho} = G_E \qquad \text{etc.}$$

$$\frac{G_M^{\omega\pi}}{[SU(3)]} = \frac{G_M^{ee}}{[SU(3)]} = \frac{G_M}{[SU(3)]} \quad \text{etc.} \tag{3.8}$$

It would also be consistent with the spirit of this work to construct Γ and then remove the kinematic momentum p (Eq. (1.2)). The corresponding relationships are different, but only by factors of the ratio of the vector meson masses. This question must be re-examined when data can distinguish between plausible possibilities.

For $e^+e^- \to VV$, due to Eqns. (3.5), (1.28), (1.29), it can be seen that the charge quadrupole moment is identically zero. The vanishing of this quadrupole moment of ρ^+, ρ^- and K^*, $\overline{K^*}$ production is a significant test of the SU(6) symmetry and depends upon the L = 0 assignment of these vector mesons. It would be true also for $e^+e^- \to \rho\rho'$ if the ρ' is an L = 0 radical recurrence of the ρ but not for an L = 2 vector meson.

We are now able to combine these results with the formalism of section 1 and compute rates for pair production of 0^- and 1^- states in terms of two unknowns $G_{E,M}$ which physically describe the relative importance of longitudinal and transverse excitation amplitudes and the overall scale.

3.1 Pseudoscalar - Pseudoscalar production

This generalises example 1 of section 1.

The pair production cross section by one photon excitation in e^+e^- collisions can be written as the sum of longitudinal and transverse photon parts. Eq. (1.1) averaged over incoming lepton spins and summed over outgoing helicities and angles gives

$$\sigma = \sigma_L + \sigma_T$$

For pseudoscalar meson pairs $\sigma_T = 0$ and

$$\sigma_L = \frac{8\pi\alpha^2}{3t} \left(\frac{p}{\sqrt{t}} \right)^3 \left| G_{E(t)} \right|^2 \left[SU(3) \right]^2 \qquad (3.10)$$

where

$$\frac{p}{\sqrt{t}} = \frac{m_1 m_2 \sinh\rho}{t} \,. \qquad (3.11)$$

(The SU(3) factors are given in Table 2.)

In the exact symmetry limit this channel is relatively uninteresting. The SU(3) Clebsch Gordan coefficients are 1 for $\pi^+\pi^-$, K^+K^-, and zero for the neutrals. Consequently this is an interesting place to study symmetry breaking.

In computing the SU(3) coefficients of Table 2 we effectively considered the photon quantum numbers to decompose as

$$\gamma = +\rho^\circ + \frac{1}{3}\omega^\circ - \sqrt{\frac{2}{3}}\,\phi^\circ \qquad (3.12)$$

where ρ^0 etc. denote the quantum numbers of the mesons, as given by magic mixing. Table 2 also shows the separate contributions of the $\rho^0\omega$ and ϕ sectors of the photon to the SU(3) coefficients. The hypothesis of vector meson dominance gives rise to the notion that these states contribute individually terms $\rho(t)$, $\omega(t)$ and $\phi(t)$ to the form factors. (In the exact symmetry limit these functions are all equal). Substituting the relevant expressions from Table 2 into the cross sections Eq. (3.10) we find for the relative production rates

$$\frac{\sigma(K^+ K^-)}{\sigma(\pi^+ \pi^-)} = \left(\frac{p_K}{p_\pi}\right)^3 \frac{\left(\frac{1}{2}\hat{\rho} + \frac{1}{6}\hat{\omega} + \frac{1}{3}\hat{\phi}\right)^2}{(\hat{\rho})^2} \qquad (3.13)$$

and

$$\frac{\sigma(K^0 \bar{K}^0)}{\sigma(\pi^+ \pi^-)} = \left(\frac{p_K}{p_\pi}\right)^3 \frac{\left(-\frac{1}{2}\hat{\rho} + \frac{1}{6}\hat{\omega} + \frac{1}{3}\hat{\phi}\right)^2}{(\hat{\rho})^2} \qquad (3.14)$$

the latter ratio being identically zero in the exact symmetry limit[10].

A plausible and oft quoted model for $\hat{v}(t)$ is

$$\hat{v}(t) = \frac{m_v^2}{m_v^2 - t} \qquad (3.15)$$

where m_v is the mass of the vector meson. This is probably a reasonable model in the low t region. It should be remembered however that contributions from higher mass states can in principle

make considerable differences to this simple form.[+] However, in this model Eq. (3.13) becomes identical with Eq. (3) of reference 20 and in excellent agreement with the Frascati data. The comparison is shown in fig. (1a) along with the exact symmetry ($\hat{\rho} = \hat{\omega} = \hat{\phi}$) prediction. The predictions for $\sigma(K^0\bar{K}^0)/\sigma(K^+K^-)$ are shown in fig. (1b). It would be interesting to compare this with data away from the ϕ resonance region.

3.2 Vector-Pseudoscalar production

This generalises example 3 of section 1. In this case one has $\sigma_L = 0$

$$\sigma_T = \frac{4\pi\alpha^2}{3m_v^2}\left(\frac{p}{\sqrt{t}}\right)^3 \left|G_M(t)\right|^2 \left[SU(3)\right]^2 \qquad (3.16)$$

m_v is the vector meson mass. The relative production rates of (V,P) as against (P,P) is not give by $SU(6)_w$. However, comparing $\omega^0\pi^0$ with $\pi^+\pi^-$ production gives, using Table 2

+ Examination of $\pi^+\pi^-$ data suggests that the higher states and tail effects merely cause a slower fall-off in t than a simple pole form would suggest. There are no significant structures seen for $t < 9\,(GeV)^2$ (3, 20, 21).

$$\frac{\sigma(\omega^0 \pi^0)}{\sigma(\pi^+\pi^-)} = \frac{1}{2}\left(\frac{p_\omega}{p_\pi}\right)^3 \cdot \frac{t}{m_\omega^2}\left|\frac{G_M(t)}{G_E(t)}\right|^2 \qquad (3.17)$$

This ratio yields a direct determination of $\left|G_M(t)/G_E(t)\right|$.

Within the vector meson dominance framework one can obtain the equation

$$G_M(t) = 2G_E(t) \qquad (3.18)$$

which is equivalant to the more familiar relation

$$\left(g_{\rho\omega\pi}/g_{\rho\pi\pi}\right)^2 = 4/m_\omega^2 \qquad (3.19)$$

and successfully correlates the ρ and ω decay widths (22, 23). Although, as we shall see, Eq. (3.18) is not consistent with $SU(6)_w$ near to the vector meson pair production threshold it is interesting to use it to compute $\sigma(\omega^0\pi^0)$ from Eq. (3.17) and the data on $\sigma(\pi^+\pi^-)$. Fig. 2 shows this calculation and compares it with data (3, 24, 25, 26) on $\sigma(\pi^0\pi^0\pi^+\pi^-)$ which, near to threshold, is dominated by $\omega^0\pi^0$ production. At low t the agreement is satisfactory, at large t other quasi two body channels can contribute, ($\rho^+\rho^-$, πA_1 for example.) Our $\rho^+\rho^-$ production estimate is also shown in fig. 2 and this alone does not explain the discrepancy.

Using the same broken symmetry arguments as before the cross sections for vector pseudoscalar production are shown in fig. 3.

3.3 Vector Vector Production

This generalises example 5 of section 1.

Pairs of vector mesons can be produced by both longitudinal and transverse photons, and the assumption of $SU(6)_w$ symmetry was seen (Eq. (3.5), 3.6) to again restrict the production to the charge monopole and magnetic dipole modes

$$\sigma_L = \frac{8\pi\alpha^2}{t}\left(\frac{p}{\sqrt{t}}\right)^3 \left| G_E(t) \right|^2 \left[SU(3)\right]^2 \qquad (3.20)$$

$$\sigma_T = \frac{8\pi\alpha^2}{3m_v^2}\left(\frac{p}{\sqrt{t}}\right)^3 \left| G_M(t) \right|^2 \left[SU(3)\right]^2 \qquad (3.21)$$

Near to the production threshold $SU(6)_w$ gives the constraint

$$G_E(t) = G_M(t) \qquad (3.22)$$

Although this is probably not true well below threshold (c.f. Eq. 3.18) we take it to be a good enough approximation to make useful estimates of the low energy production. The transverse cross section (Eq. (3.21)), and hence $G_M(t)$, dominates this vector pair production. Taking the same magnetic form factor which fitted $\omega^0\pi^0$ production then fig. 4 shows our estimates of vector-vector pair production cross sections.

All of these calculations can be easily generalised to include charm. The extension of the SU(3) coefficients to SU(4) is given

in Table 3 for the scheme where the photon has a sector containing a ϕ_c^o (a bound state of a charmed quark, charge $^2/_3$ e, and its antiparticle.)

3.4 $e^+e^- \rightarrow 4\pi$ and the $\rho'(1250)$

We saw in section 3.2 and fig. 2 that the $e^+e^- \rightarrow \pi^o\ \pi^o\ \pi^+\ \pi^-$ channel while in fair agreement with $\pi^o\omega$ near to threshold showed substantial enhancement for larger values of t. It is interesting experimentally and theoretically to clarify the mechanisms contributing here (see also Felicetti ref. 3).

Three possibilities suggest themselves:

(i) There is substantial $\pi^{\mp} A_1^{\pm}$ production contributing some 50nb at $\sqrt{t}$ = 1.2 GeV. Admittedly the A_1 can be produced below its nominal mass value but it is very hard to imagine such a large cross section at such an energy. Furthermore one would then expect a similar signal in the $\pi^{\mp} A_1^{\pm} \rightarrow \pi^+\ \pi^-\ \pi^+\ \pi^-$ channel whereas this cross section (3) at $\sqrt{t}$ = 1.2 GeV is consistent with zero.

(ii) $G_M(t)$ is 2.5 times as big as the simple vector dominance model.

This gives a reasonable description of all the Frascati data though one might be concerned about the less good agreement with the ACO low energy data (26) ($\sqrt{t} \leq$ 1.1GeV in fig. 5). Improved data with reduction in errors could rule out this interpretation and data

between $t = 1.5$ and 1.8 GeV would be of interest to see if the $\rho^+\rho^-$ threshold behaviour is visible.

Such a large $G_M(t)$ will also mean that the $\pi^+\pi^-\pi^0\pi^0$ mode is about 10 nb at $\sqrt{t} = 3$ GeV and so some 40% of σ_{TOTAL} ($e^+e^- \rightarrow$ hadrons). If the $\psi(3.1)$ has G parity = -1 then the 4π decays can arise only from the sequence $\psi \rightarrow \gamma \rightarrow 4\pi$. The $2\pi^+2\pi^-$ mode has been isolated and is consistent with such a mechanism[27]. A comparison with $\pi^+\pi^-2\pi^0$ would be interesting to see if this latter is of order 10 times the $2\pi^+2\pi^-$.

The $\pi^+\pi^-\pi^0$ cross section arising from $\pi\rho$ production is $^1/_3$ of the $\pi^0\omega$ cross section. Hence, if a large magnetic form factor is responsible for the large $\pi^+\pi^-\pi^0\pi^0$ cross section we would anticipate this three pion cross section to be some 15 nb at $\sqrt{t} = 1.2$ GeV falling to some 5 nb by $\sqrt{t} = 2$ GeV.

(iii) <u>There is a $\rho'(1250)$ resonance which couples to the $\pi^0\omega$ channel</u>

At $\sqrt{t} \simeq 1.2$ GeV - 1.5 GeV the shape of the channel cross section will differ from the previous example and include a resonance peak. An example is shown in fig. 5 where the similarities and differences with the previous example are highlighted.

Unless there is also an ω' state of similar mass then the 3π channel need have no enhancement (unlike the case in example (ii) above.)

The further investigation of these and related phenomena appears worthwhile as the question whether $\epsilon'(1250)$ and $\epsilon''(1600)$ are resonance states is of much importance for many theoretical schemes. Improved data at small t would be very useful as there are few two body channels and one could hope to settle the resonance or threshold interpretation.

4. The production of a pion with another meson

Another readily identifiable quasi two meson event will be a single pion (or Kaon) recoiling against some quasi one body state. The $SU(6)_w$ results of Eq. (2.3), (2.4) simplify for a state R and 2 a pseudoscalar as follows:

(i) R with intrinsic spin $S_1 = 0$

Here $S_z = 0$ and so $W = 1$. One finds at once

$$\Gamma'_{10} = A_{0L}\,\delta_{S_1 L} \quad [SU(3)] \tag{4.1}$$

$$\Gamma'_{00} = \alpha_{0L}\,\delta_{S_1 L} \quad [SU(3)] \tag{4.2}$$

The sequence with $S_1 = 0$ always has unnatural parity.

(ii) R with intrinsic spin $S_1 = 1$

When $S_z = 1$ then $W_1 = 1$; $S_z = 0$, $W_1 = 0$.

$$\Gamma'_{10} = \left\{ \left[B_{0L} \langle L,\ 1, 0\text{-}1,\ | S_1 \text{-} 1 \rangle + D_{0L} \langle L\ 1, \text{-}2\ 1\ | S_1 \text{-} 1 \rangle \frac{1}{\sqrt{2}} \right. \right. \\ \left. \left. + C_{0L} \langle L, 1, \text{-}1\ 0\ | S_1 \text{-} 1 \rangle \right\} \right] [SU(3)] \tag{4.3}$$

Note the general result of section 1 example 4 that when R has natural parity ($S_1 = L \pm 1$, $\mathcal{S}_1 = 1$).

The t dependence of these helicity amplitudes is in the reduced matrix elements $B_{0L}(t)$ etc. It is to be expected that this t dependence will be governed not only by the general kinematic structure of section 1 but also by L, and for example $A_2(L=1),\pi$ and $A_2'(L=3),\pi$ can be expected to have different behaviour near to threshold. These features could be a test of the $L \otimes \mathcal{S}$ substructure of a hadron.

A similar story is found in $ep \to eS_{11}(1550)$ and $eD_{13}(1520)$ which are "brothers" (L=1) in the quark model. See F. Foster in ref. 26.

4.1 Threshold behaviour in $e^+e^- \to R\pi$ and violations of scaling.

If R is a natural parity state with spin S_1, then as shown in example (iv) of section 1

$$\Gamma'_{10} = (-1)^{S_1} \frac{S_1!\, 2^{S_1}}{\sqrt{2(2S_1)!}} \left[\sinh\left(\tfrac{1}{2}\rho\right)\cosh\left(\tfrac{1}{2}\rho\right)\right]^{S_1} T_0^{S_1}(t) \qquad (4.9)$$

and, for the $e^+e^- \to R\pi$ cross-section

$$t\frac{d\sigma}{dx} = \frac{2\pi\alpha^2}{3t}\left(x^2 - \frac{4m_\pi^2}{t}\right)^{1/2} |\Gamma'_{10}|^2 \qquad (4.10)$$

$x \simeq 1 - m_R^2/t$ and for fixed m_R, $x \to 1$ as $t \to \infty$, the spin averaged cross section decreases as t^{-N} with N some number independent of M_R and probably related to the number of quarks contained in the state R[28].

As $x \longrightarrow 0$, $t \longrightarrow t_{\text{threshold}}$. The produced π and the state R are nearly at rest (hence only one dimension characterises the configurations[29]). The behaviour of $t\frac{d\sigma}{dx}$ is now predominantly governed by the threshold behaviours - the rapidity dependent factors in eq.(4.9).

The typical shape of $t\frac{d\sigma}{dx}$ for a given M_R can be expected to be as shown in fig. 6. Note that the threshold behaviour is crucially spin S_1 dependent whereas the high t behaviour is supposed[28] to be spin(S_1) independent. The behaviour exhibited in the figure is essentially the same

as that of fig(3) for $\sigma(e^+e^- \to \pi^0\omega)$.

If we now repeat the exercise for a state of higher spin then since higher spins tend to be associated with higher mass M_R which, for given x, in turn yields higher t, a short calculation shows the tendency of $t\frac{d\sigma}{dx}$ to increase at small x as M_R increases (so long as there is no dramatic counteracting suppression in the $T_o^S(t)$). Similar results obtain for the unnatural parity states after more lengthy calculations. Clearly a question for experiment to decide is whether the $T_o^S(t)$ are strongly or weakly dependent on S near to threshold.

If it was the case that $e^+e^- \to \pi X$ was dominated by quasi two body production πR then, since for each state R one would expect the behaviour of fig (6), such behaviour would also be expected in the inclusive data. Although such effects could be obscured by other processes, even other quasi two body channels (e.g. $e^+e^- \to \rho^+\rho^- \to \pi^0\pi^0\pi^+\pi^-$), it is interesting to note that such behaviour is seen in the inclusive data[30]. It is tempting to suggest that the failure to see scaling at small x is due to the importance of threshold phenomena in this domain.

Although this picture of scaling violation at small x might not be the whole truth about the observed violations we would stress that threshold phenomena should not be cavalierly ignored. In this connection it is interesting to note that in electroproduction one can be far from threshold even at small t when ν (and the produced mass) is large. The threshold for the reaction $\gamma 2 \to \bar{1}$ is at $\sinh\frac{1}{2}\xi = 0$ ($t = (m_1 - m_2)^2$); not at t=0. The physical regions in t, ν space are shown in fig. 7 where $2m_1\nu = m_2^2 - m_1^2 - t$. The magnitude of the cross section can be imagined superimposed on the kinematic figure yielding a three dimensional plot. A slice through this along the axis of constant m_1 and m_2 will result in a cross section that can be anticipated to be as in fig (8). The threshold region for $t \leq (m_1 - m_2)^2$ can be observed in decays involving lepton pair emission. In particular however it should be noted that this threshold region, where scaling violation can again be anticipated, need not encroach upon the electro production region, $t < 0$.

5. Conclusions and Summary of Experimental Questions.

Even before the recent exciting discoveries[2] it was clear that studies of exclusive channels in e^+e^- annihilation would be an interesting and fruitful field.

Our aim in this paper has been to formulate a general description of quasi two body production in e^+e^- annihilation. The definitions of constraint free form factors in section 1 are for arbitrary spin combinations and one can immediately write down the form of the cross section for any chosen situation. Previous work[4-7] had only discussed specific states and no other explicit general framework is known to us.

The $SU(6)_W$ constraints that obtain for these various helicity amplitudes are given in section 2 for arbitrary meson pairs. Combination of these results with the formalism of section 1 enables one to obtain relations among cross sections for production of members of the same multiplet.

The cases of immediate relevance - the production of 0^- and 1^- states - are discussed in detail in section 3. Hopefully in the not too distant future it will be worthwhile making a similar extensive discussion for the production of baryon as well as higher meson multiplets. This is straightforward within the framework presented here.

If charmed states associated with the new mesons are produced above $t \approx 16\ GeV^2$ then the extension of section 2, in particular table 3, can be used in rate estimates.

Within the general kinematic and $SU(6)_W$ symmetry structure we have attempted to classify some of the questions which may be answered in the near future. As the content of this paper has been rather wide ranging we list here what we regard as the most important questions.

(1) After the threshold factors of section 1 have been removed what is the t dependence of the form factors? States of high spin cannot have form factors that are naively vector dominant since unitarity bounds would be violated.

(2) How does the t dependence of the form factors for $R\pi$ vary as a function of spin and normality of the state R?

The answer to this question is significant for parton models and related ideas; for understanding the t dependence of the total and x dependence of the inclusive cross section. The answer will severely constrain models of hadron substructures and yield insight into the pair production dynamics. An immediate question is the vector meson dominance of the form factors in (VP) and (VV) production.

3. Is $\rho^+\rho^-$ production compatible with vanishing quadrupole moment? A non vanishing moment would have serious implications for $SU(6)_W$ schemes.

Is σ_L/σ_T for $\rho^+\rho^-$ directly related to $\sigma(\pi\pi)/\sigma(\pi\omega)$? This is expected in the symmetry framework and information on this would determine $|G_E(t)/G_M(t)|$.

4. What is the t dependence of $e^+e^- \longrightarrow \pi^+\pi^-\pi^0\pi^0$? Is the observed structure due to a ρ' (1250) or to threshold phenomena? Improved data at small t would help to settle this question as available channels for threshold phenomena are few. Data between 1.5 and 2 GeV in $\sqrt{t}$ will also be useful in order to investigate the e^+e^- threshold (section 3.4).

Finally, how large is this channel at $\sqrt{t}$=3GeV? It was suggested in section 3.4 that it could be as much as 10 nb out of the total of 25nb. Is the behaviour for $t > 1.5$ $(\text{GeV})^2$ smooth or are there further threshold and/or resonance enhancements (e.g. around 1.8 to 2 $(\text{GeV})^2$ - cf. figs 2 and 5).

One of us (W.N.C.) would like to thank the S.R.C. for a travel grant and his colleague Dr. B. Pollard for discussions. We are grateful to B. Humpert, G. Kramer, A. Zichichi and members of the C.E.R.N. electromagnetic club for discussions and to J. Ellis for reading the manuscript.

1. B. Richter in XVII Int. Conference on High Energy Physics, London (1974)p. IV -37.

2. J. J. Aubert et al, Phys. Rev. Letters, 33, 1404 (1974)
J. E. Augustin et al, Phys. Rev. Letters 33, 1406 (1974)
C. Bacci et al, Phys. Rev. Letters 33, 1408 (1974), Erratum ibid 1649
G. S. Abrams et al, Phys. Rev. Letters 33, 1453 (1974)
W. Braunschweig et al, Phys. Letters 53B, 393 (1975)

3. A. Zichichi in XVII Int. Conference on High Energy Physics, London (1974), p. IV-6; F. Felicetti, ibid p. IV-10.

4. G. Kramer and T. F. Walsh, Z. Physik 263, 361 (1973).

5. G. Kramer, J. L. Uretsky and T. F. Walsh, Phys. Rev. D3, 719 (1971)

6. J. Layssac and F. M. Renard, Lett. Nuov. Cim 1, 197 (1971)
Nuovo Cimento 6, 134(1971)

7 A. M. Attukhov and I. B. Khriplovich, Sov. J. Nucl. Phys. 14, 440 (1972)

8 T. L. Trueman, Phys. Rev. 182, 1469 (1969)

9 J. L. Rosner in ref. 3 p. II-171;
S. Meshkov, ibid p. II-101; A. J. G. Hey, ibid p. II-120;
F. E. Close, ibid p. II-157.

10 H. J. Lipkin, Phys. Rev. Letters 31, 656 (1973)

11 A. R. Edmunds "Angular Momentum in Quantum Mechanics" Princeton Univ. Press. Eqn (4. 3. 1) and (3. 5. 16).
K. Gottfried, "Preludes in Theoretical Physics' North Holland.
Ed. A. De Shalit et al.

12 M. Gourdin, Hadronic Interactions of Electrons and Photons, Academic Press, Edited by J. Cumming and H. Osborn (1971).

13. F. J. Ernst, R. G. Sachs and K. C. Wali, Phys. Rev. 119, 1105 (1960)

14. J. Weyers, CERN TH1743 (1973)
F. J. Gilman, Proc. of 14th Scottish Universities Summer School in Physics 1973.

15. F. J. Gilman and M. Kugler, Phys. Rev. Letters 30 (1973) 518
A. Hey and J. Weyers, Phys. Letters 44B (1973) 263;
48B (1974) 69.
F. J. Gilman, M. Kugler and S. Meshkov, SLAC-PUB (1973) 1286
F. J. Gilman and I. Karliner, Phys. Letters 46B (1973) 426.
H. J. Lipkin NAL 73/62 (1973)

16 F. E. Close, H. Osborn and A. M. Thomson, Nucl. Phys. B77 (1974)281
F. E. Close, Nucl. Phys. B80 (1974) 269

17 H. J. Melosh, Ph. D. thesis (Caltech (unpublished); Phys. Rev. D9, 1095 (1974).

18 R. Carlitz and J. Weyers, CERN-TH-1957 (1975)

19 M. K. Gaillard, B. W. Lee and J. Rosner, Rev. Mod. Phys (1975)(to appear)

20 M. Bernardini et al, Phys. Letters 46B, 261 (1973).

21 F. M. Renard in ref. 3 pIV-16.

22 G. J. Gounaris, Phys. Letters 51B (1974) 491

23 F. M. Renard, Proc. of 8th Rencontre du Moriond
M. Greco and Y. N. Srivastara, LNF 74/52 (1974)

24 K. Strouch, Proc. of 6th Int. Symposium on Electron and Photon Interactions at High Energies, North Holland 1973.

25 G. Cosme et al, paper 4 in ref. 24 (ÄCÖ)

26 M. Conversi et al Phys. Letters 52B, 493 (1974)

27 Private communication and F. J. Gilman SLAC-PUB Feb (1975)

28 F. Foster p. II-163 of ref. 3.

29 F. E. Close and F. J. Gilman, Phys. Letters 38B, 541 (1972)
F. E. Close, F. J. Gilman and I. Karliner, Phys. Rev. D6, 2533 (1972)

30 S. J. Brodsky and G. Farrar, Phys. Rev. Letters 31, 1153 (1973)
and SLAC-PUB-1473 (1974).
V. Matveev, R. Muradyan and A. Tavkhelidze, Lett. Nuov. Cim. 7, 719 (1973)

31 D. Amati and S. Fubini, Phys. Letters 49B, 293(1974)

32 B. Richter, p IV-37 of ref. 3.

TABLE 1

$$\langle 1, W_z | \sigma_+ | 1, W_z - 1 \rangle = \langle 1, W_z | \sigma_- | 1, W_z + 1 \rangle = 1/\sqrt{2}$$

$$\langle 1, W_z | \sigma_z | 1, W_z \rangle = W_z$$

$$\langle 1, 1 | \sigma_+ | 0, 0 \rangle = \langle 0, 0 | \sigma_- | 1, 1 \rangle = -1/\sqrt{2}$$

$$\langle 1, 0 | \sigma_z | 0, 0 \rangle = \langle 0, 0 | \sigma_z | 1, 0 \rangle = 1$$

$$\langle 1, -1 | \sigma_- | 0, 0 \rangle = \langle 0, 0 | \sigma_+ | 1, -1 \rangle = 1/\sqrt{2}$$

Magnitudes of spinor matrix elements relevant to eqs. 2.3 and 2.4.

TABLE 2

$\gamma = +\rho^0 + \frac{1}{3}\omega - \frac{\sqrt{2}}{3}\phi$, where ρ^0, ω and ϕ denote the quantum numbers of the mesons in magic mixing. This table gives the $[SU(3)]$ coefficients of the text and the individual contributions of the meson sectors of the photon.

		ρ	ω	ϕ	$[SU(3)]$
$\pi^+\pi^-$	e^+e^-	1	0	0	1
K^+K^-	$K^{*+}K^{*-}$	$1/2$	$1/6$	$1/3$	1
$K^0\bar{K}^0$	$K^{*0}\bar{K}^{*0}$	$-1/2$	$1/6$	$1/3$	0
$\pi^+\rho^-$	$\rho^+\pi^-$	0	$1/3$	0	$1/3$
$\eta\omega$	$\pi^0\rho^0$	0	$1/3$	0	$1/3$
$\eta\rho^0$	$\pi^0\omega$	1	0	0	1
K^+K^{*-}	$K^{*+}K^-$	$1/2$	$1/6$	$-1/3$	$1/3$
$K^0\bar{K}^{*0}$	$K^{*0}\bar{K}^0$	$-1/2$	$1/6$	$-1/3$	$-2/3$
$\eta\phi$		0	0	$-2/3$	$-2/3$

TABLE 3

An extension of table 2 to the possible charmed mesons.

$$\gamma = +\rho^0 + \frac{1}{3}\omega - \frac{\sqrt{2}}{3}\phi + \frac{2\sqrt{2}}{3}\phi_c$$

where ρ^0, ω, ϕ and ϕ_c denote the quantum numbers of the mesons in the extended magic mixing scheme. Our notation follows that of ref. 19.

		ρ^0	ω	ϕ	ϕ_c	[SU(4)]
F^+F^-	$F^{*+}F^{*-}$	0	0	1/3	2/3	1
D^+D^-	$D^{*+}D^{*-}$	1/2	-1/6	0	2/3	1
$D^0\bar{D}^0$	$D^{*0}\bar{D}^{*0}$	-1/2	-1/6	0	2/3	0
F^+F^{*-}	$F^{*+}F^-$	0	0	-1/3	2/3	1/3
D^+D^{*-}	$D^{*+}D^-$	-1/2	1/6	0	2/3	1/3
$D^0\bar{D}^{*0}$	$D^{*0}\bar{D}^0$	1/2	1/6	0	2/3	4/3
$\eta_c\phi_c$		0	0	0	4/3	4/3

FIGURE CAPTIONS

Fig. 1. Predictions for (a) K^+K^-: $\pi^+\pi^-$ and (b) $K^0\bar{K}^0$: K^+K^- production rates as a function of t with form factors in broken SU(3) (upper curves) and exact symmetry (lower curves). In the exact symmetry $K^0\bar{K}^0$ production vanishes. The data point is from ref. 20.

Fig. 2. Comparison data for $\sigma(e^+e^- \rightarrow \pi^-\pi^+\pi^0\pi^0)$ Felicetti ref. 3) and the $\pi^0\omega$ (- - -) and $\rho^+\rho^-$ (———) predictions in SU(6) with vector dominance of $G_M(t)$ (see text, section 3). The sum of these curves is given by the solid line

Fig. 3a. Contribution to $R = \frac{\sigma(e^+e^- \rightarrow \text{hadrons})}{\sigma(e^+e^- \rightarrow \mu^+\mu^-)}$ arising from pseudoscalar-vector meson pair production. The - - - is for non strange states ($\pi\rho$, $\pi\omega$, $\eta\rho$, $\eta\omega$) and ——— is with inclusion of strange states ($K K^*$.) In the quark parton model the ratio $R_{\text{nonstrange}}$: R_{total} = 5:6. If one displaces the curves to allow for mass breaking (align the maxima) then the pseudoscalar-vector meson production generates 4. 5:6 for this ratio. The peak at $t = 1.5\ (\text{GeV})^2$ is from πV alone, the addition of ηV generates the peak at t=2. 5. The $\eta' V$ and $\eta\varphi$ con tributions are expected to be small and so this is compatible with the parton model prediction. These curves may be converted to cross sections in nb by multiplying by $88/t\ (\text{GeV})^2$.

Fig. 3b. As in 3a but for vector-vector production ($- - - \rho^+\rho^-$, $\text{——}\ e^+e^-$ and K^*K^*). The strange meson production is relatively more important than in 3a due to the relative proximity of the φ pole.

Fig. 4 R for pseudo-scalar vector and vector-vector non strange mesons including a $\rho'(1250)$ (as in fig. 5) in the magnetic but not in the electric coupling. If $\rho''(1600)$ couples to these channels then a substantial fraction of R_{total} is coming from these quasi two body channels.

Fig. 5. Data on $\sigma(e^+e^- \to \pi^+\pi^-\pi^0\pi^0)$ (as fig. 2). Curves are - - - G_M is 2.5 times as big as the simple vector dominance model, ——— The vector dominance model of fig. 2 with the addition of a $\rho'(1250)$ with width 150 MeV.

Fig. 6. Qualitative shapes of $t\frac{d\sigma}{dx}(e^+e^- \to \pi R)$ for a given mass M_R plotted against $x = 1 - M_R^2/t$. (after eqn. 4.10). The $x \to 0$ reflects threshold behaviour and is dependent in particular upon the spin of the state R. As $x \to 1$ one probes the $t \to \infty$ behaviour. The upper curve is for a state R with mass and spin greater than for the state R (lower curve).

Fig. 7. Physical regions for various "photon" processes

$2m_1\nu \equiv m_2^2 - m_1^2 - t$ and $m_1 = m_\pi$, $m_2 = m_x$.

Fig. 8. The qualitative behaviour as a function of t to be expected of cross-sections for photon $+ \bar{2} \to 1$ and photon $\to 1, 2$ where 1 and 2 have masses $m_{1,2}$ and where t is the squared photon mass.

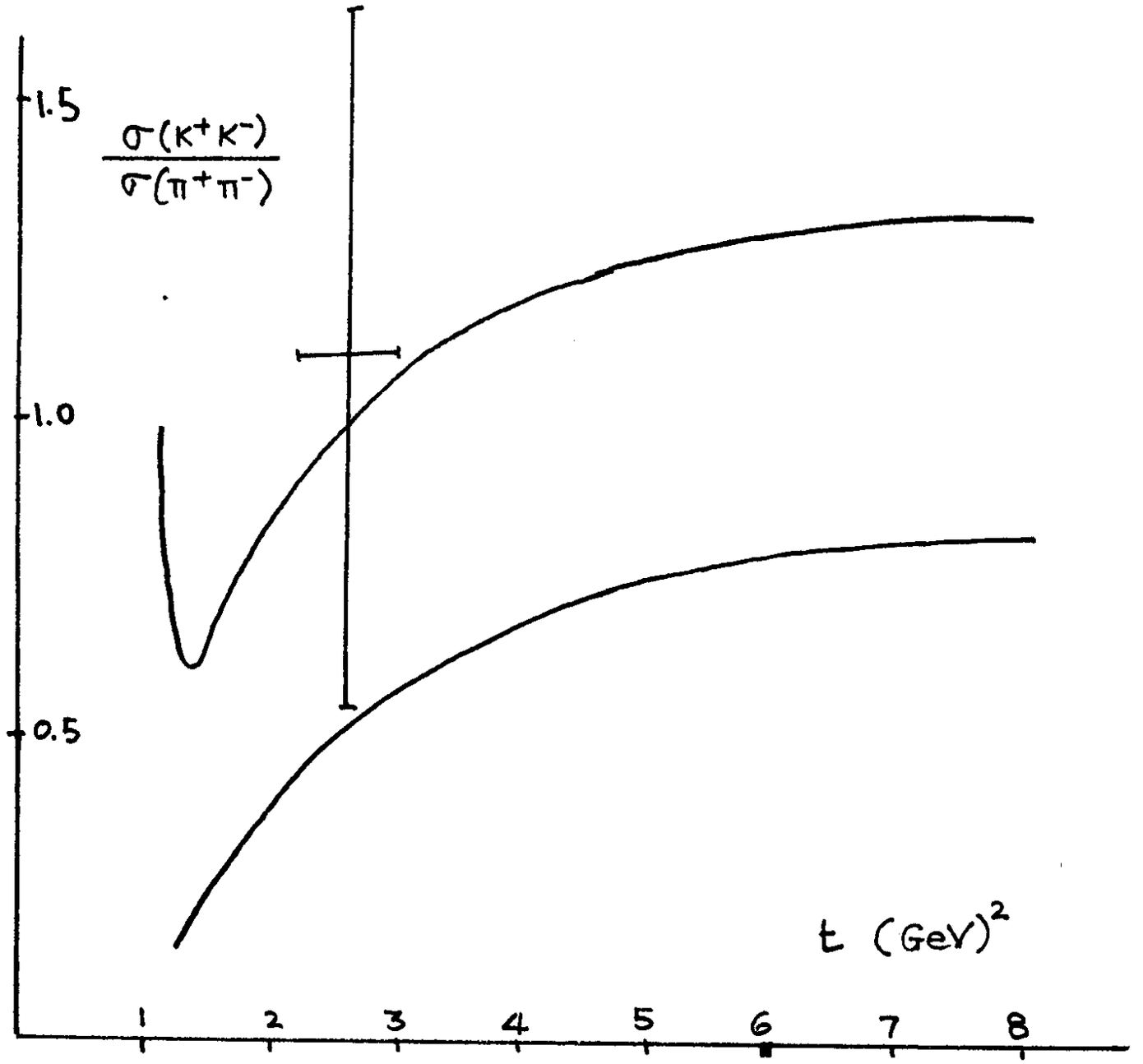
1.5
$\frac{\sigma(K^+K^-)}{\sigma(\pi^+\pi^-)}$
1.0
0.5
t (GeV)^2
1
2
3
4
5
6
7
8

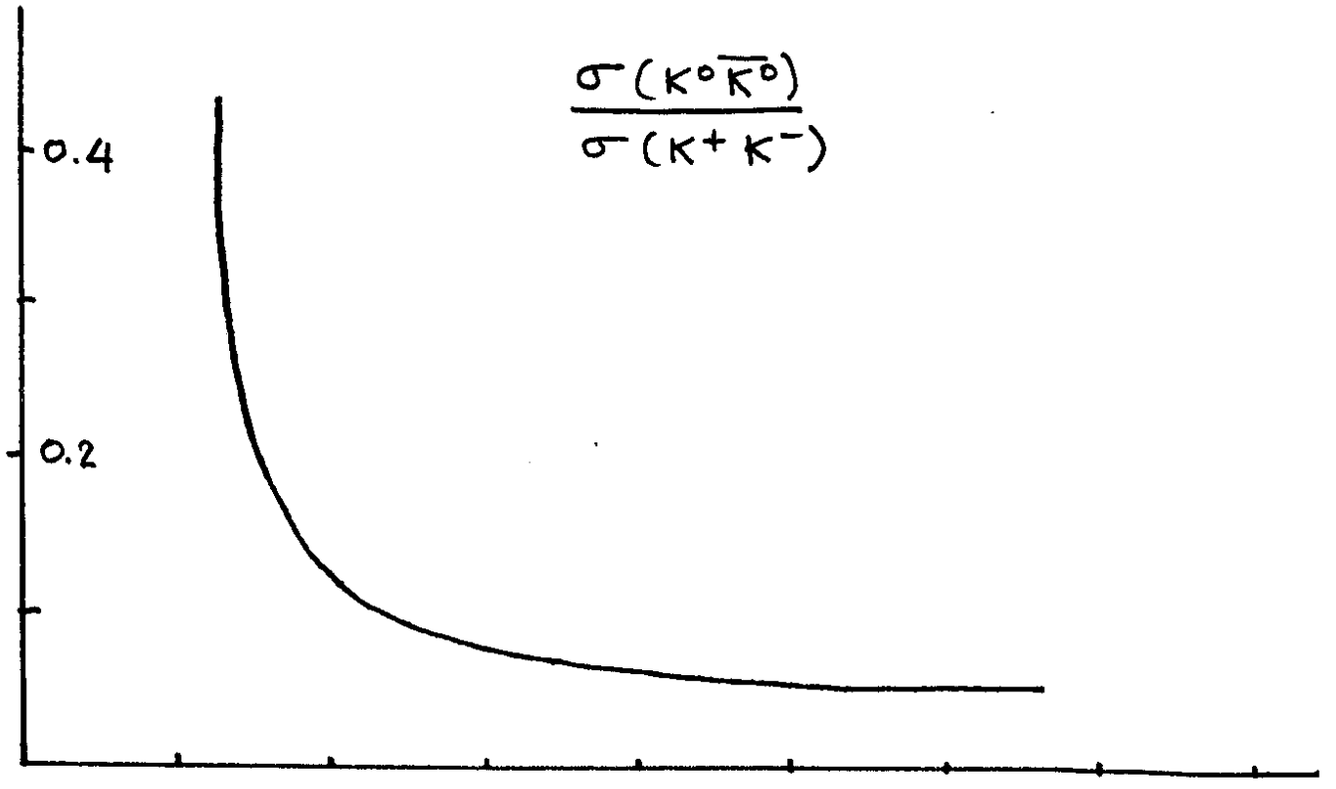
$\frac{\sigma(K^0\bar{K}^0)}{\sigma(K^+K^-)}$
0.4
0.2

Fig 1

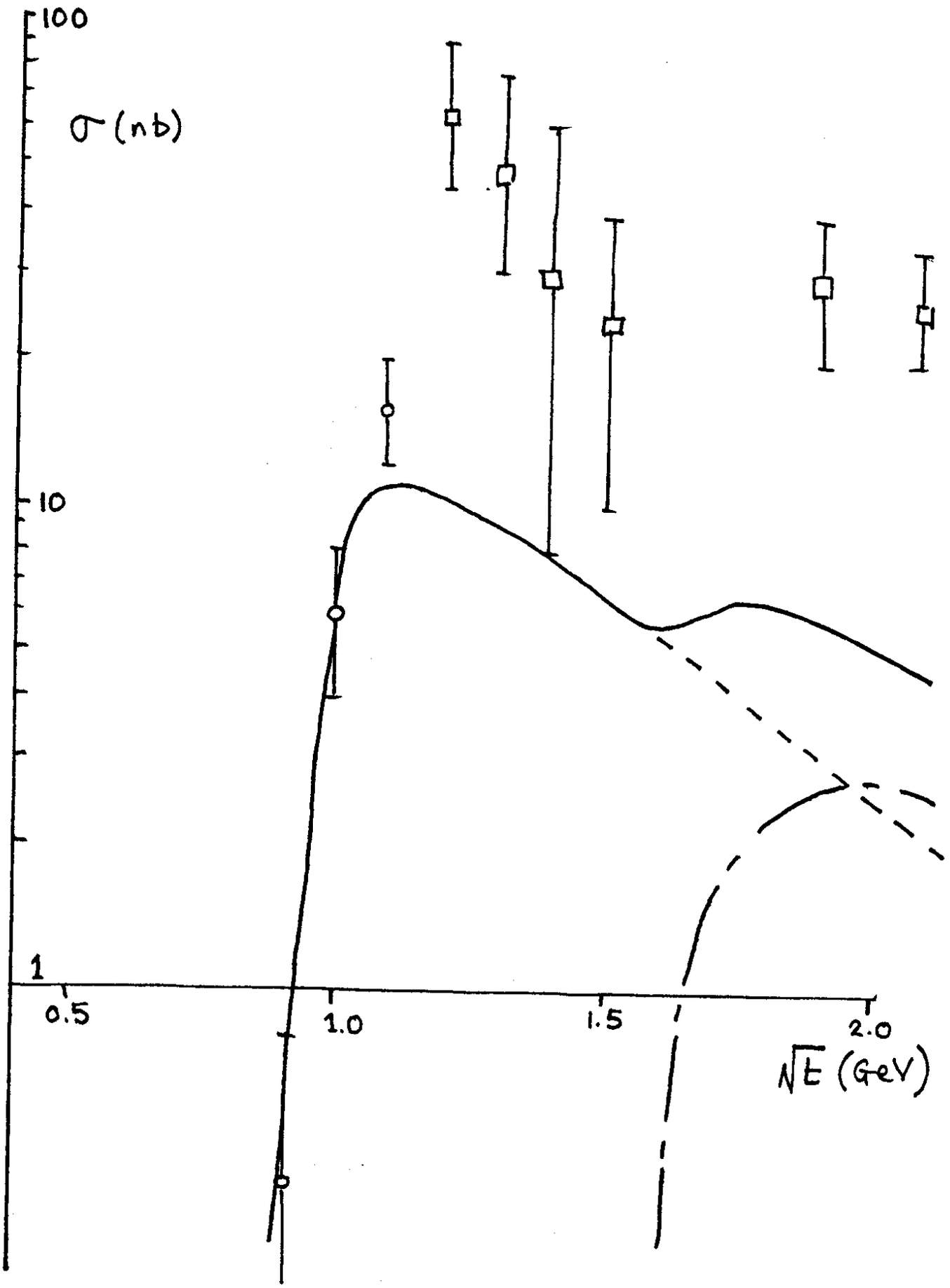

Fig 2

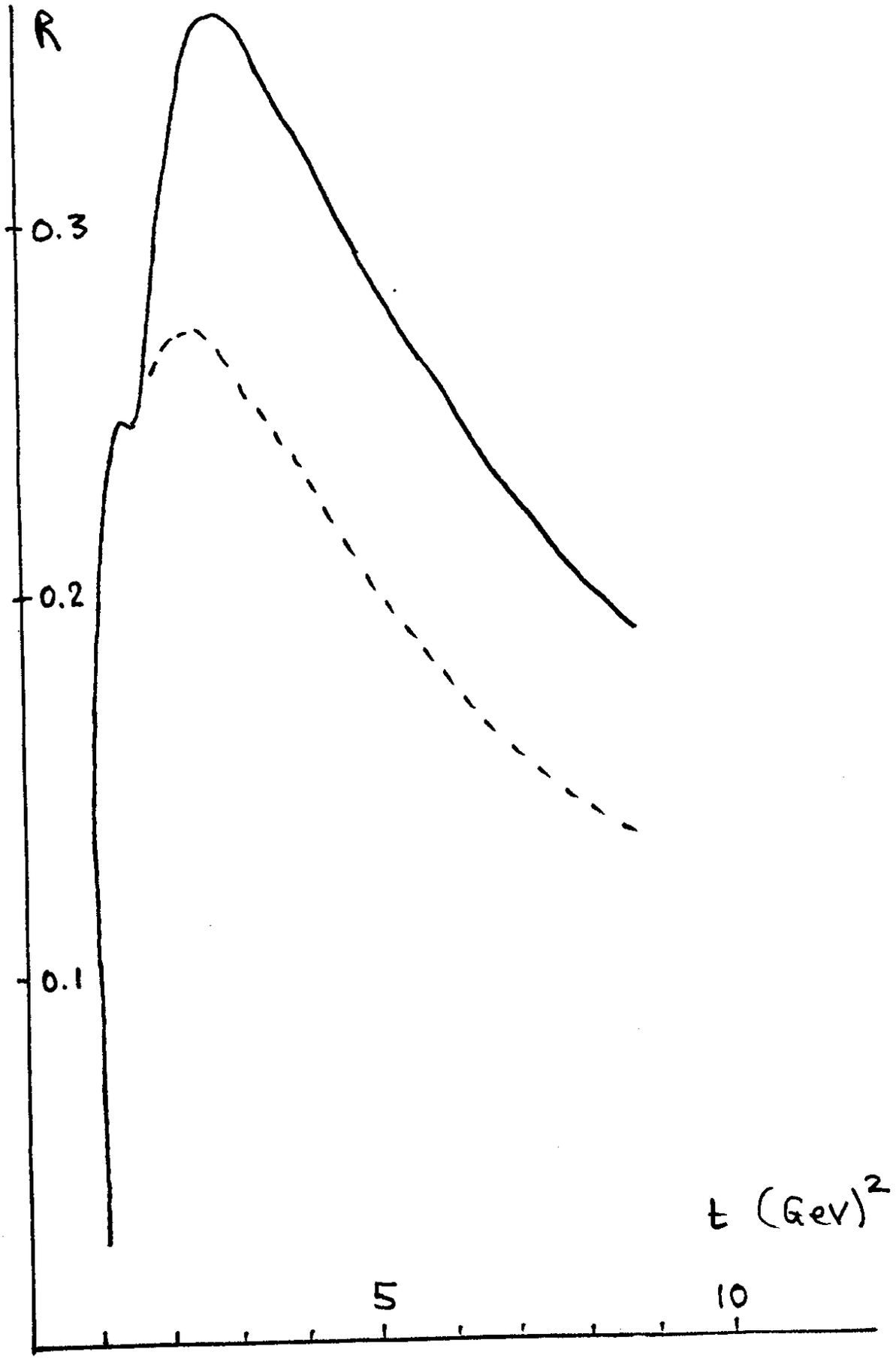

Fig 3a.

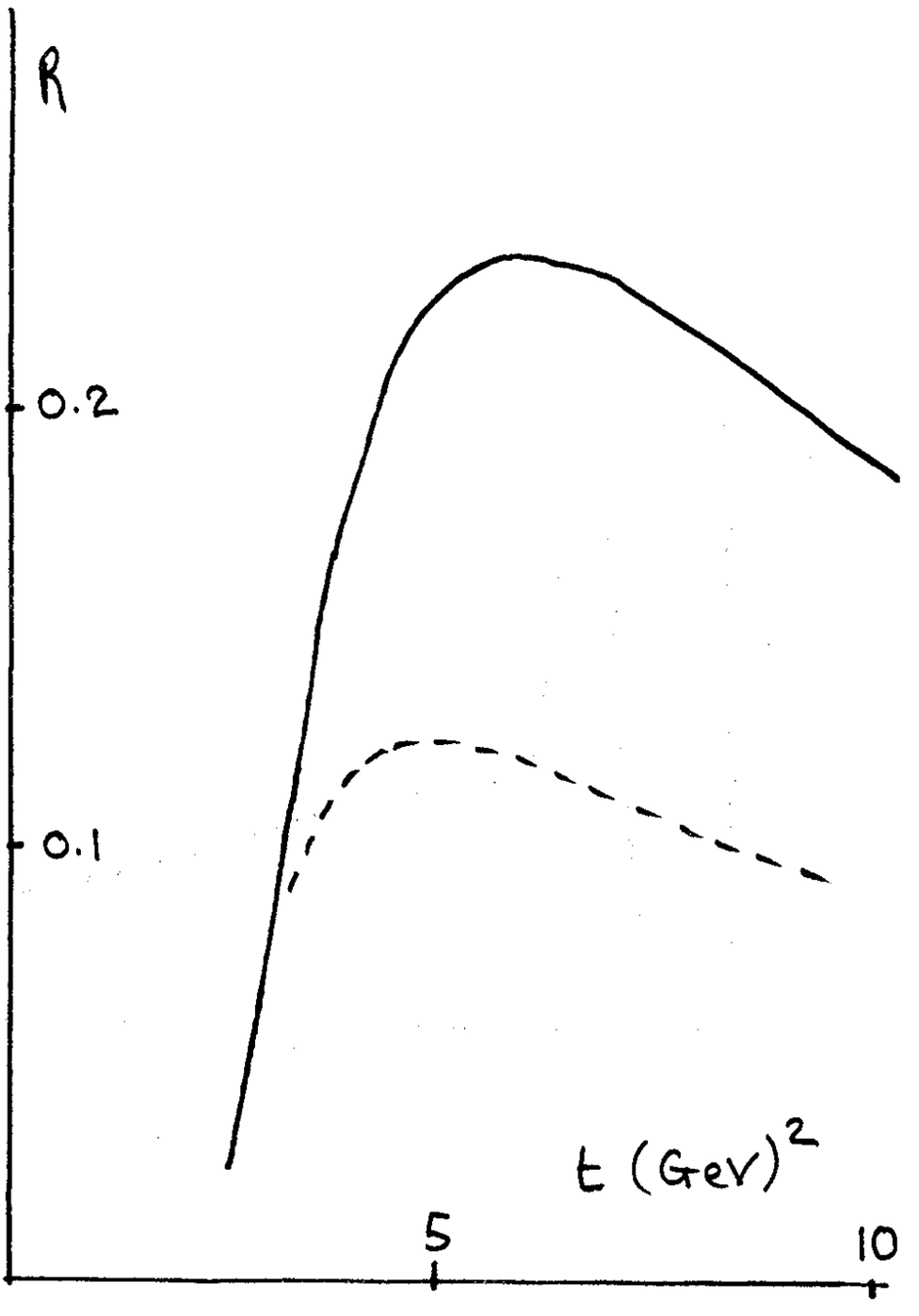

Fig 3 b

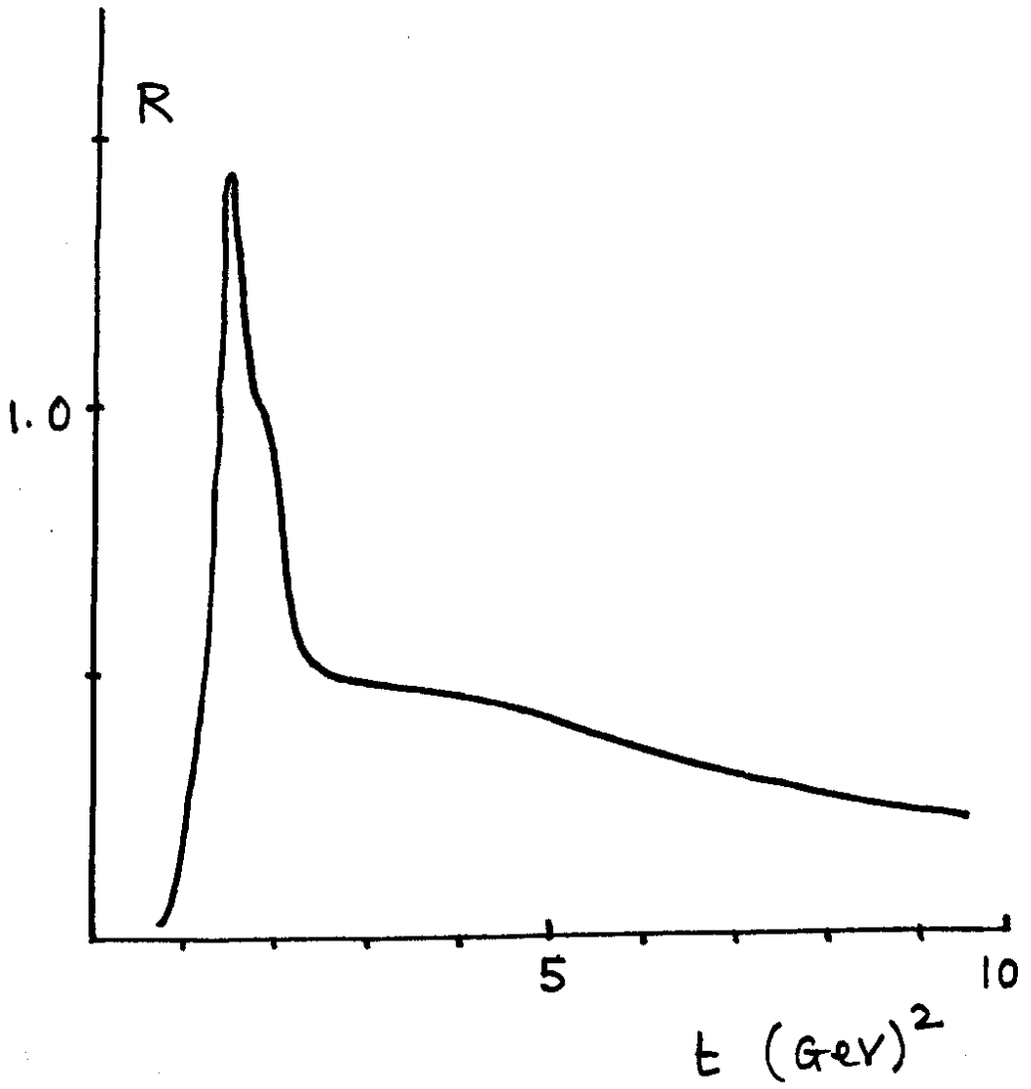

Fig 4

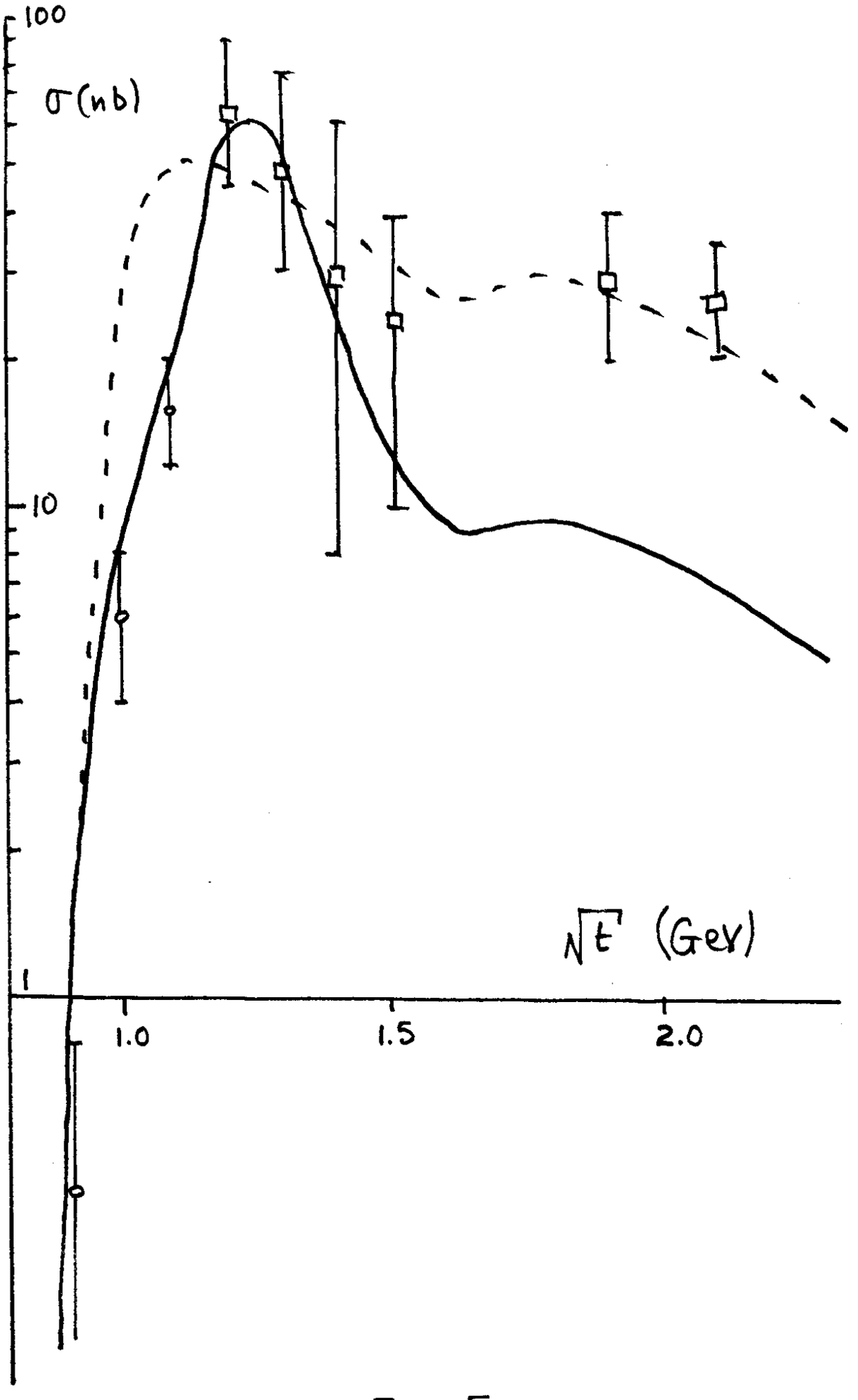

Fig 5

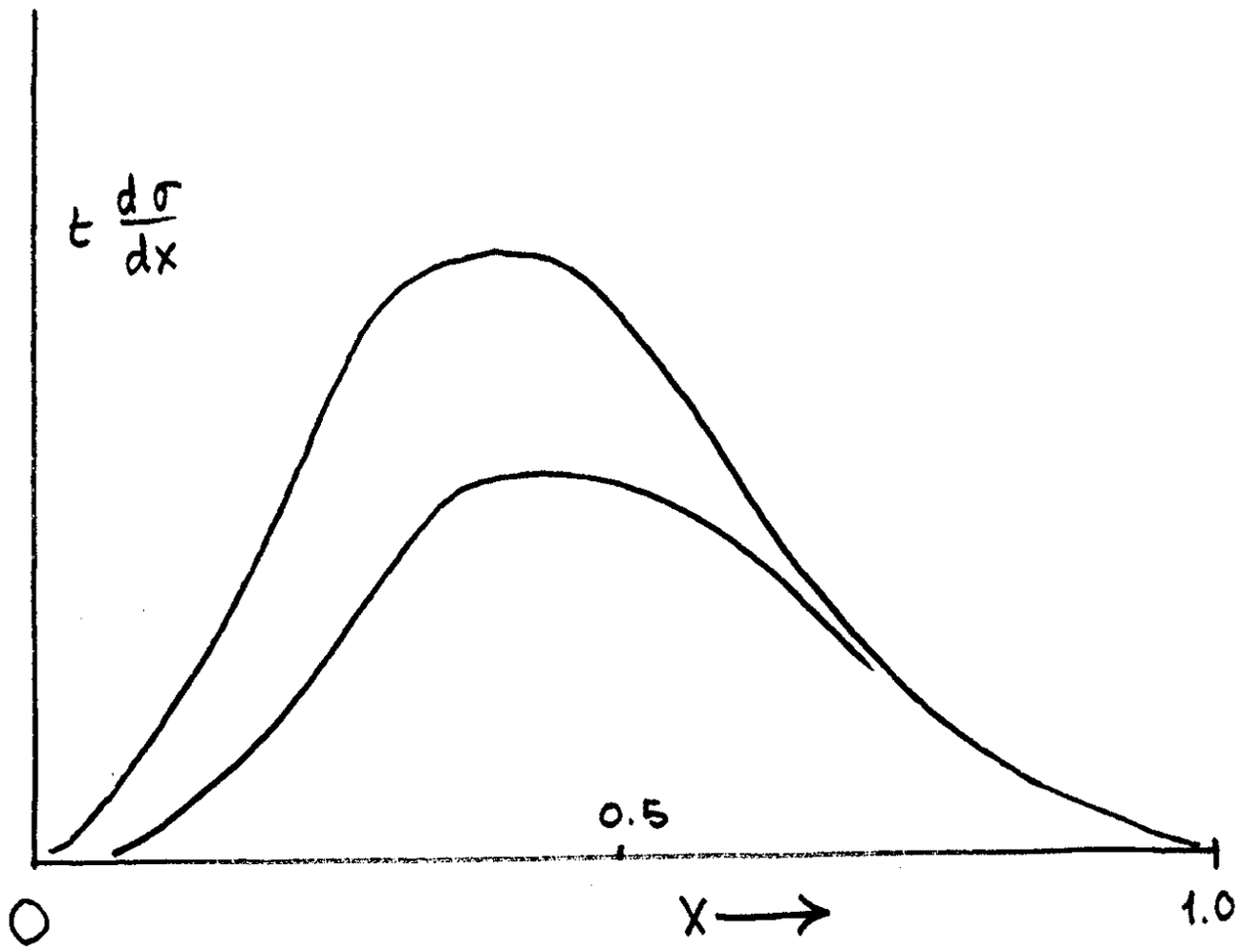

Fig 6

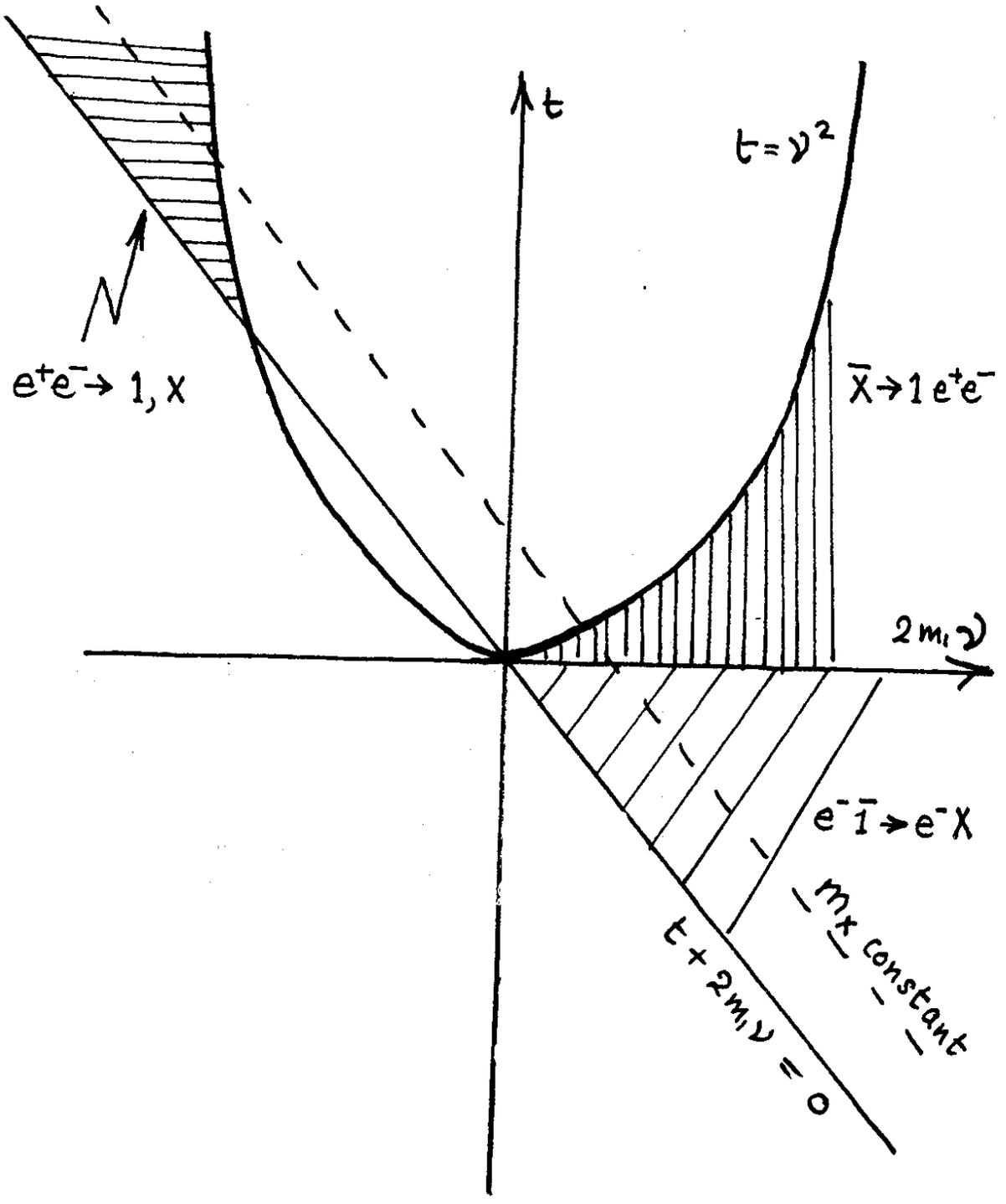
t
$t = \nu^2$
$e^+e^- \to 1, X$
$\bar{X} \to 1\, e^+e^-$
$2m_1\nu$
$e^-\bar{1} \to e^-X$
m_X constant
$t + 2m_1\nu = 0$

Fig 7

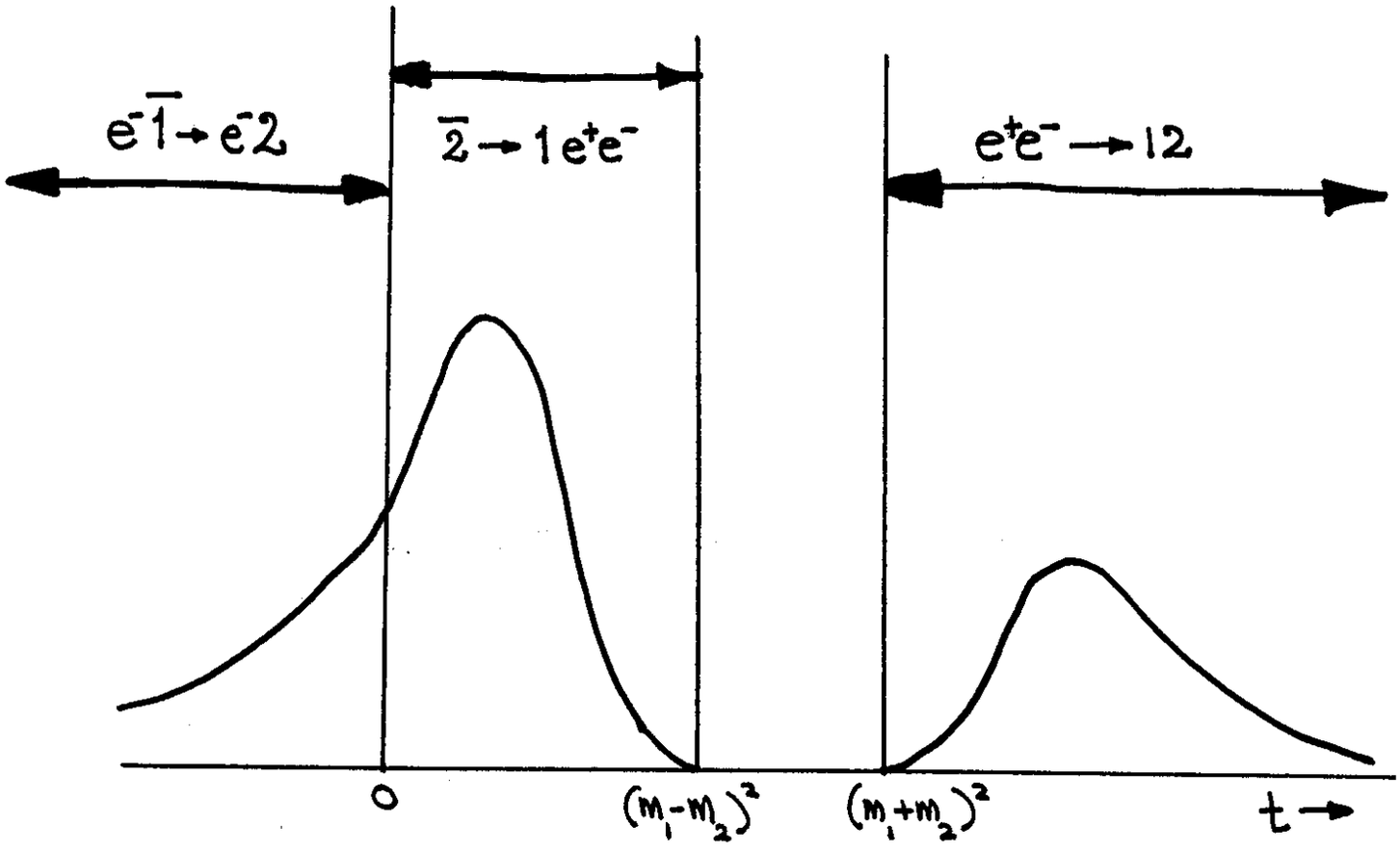

Fig 8